

## Pure-Absorption-Phase Dynamic-Angle Spinning

K. T. MUELLER, E. W. WOOTEN, AND A. PINES\*

*Materials Sciences Division, Lawrence Berkeley Laboratory, 1 Cyclotron Road, Berkeley, California 94720; and Department of Chemistry, University of California, Berkeley, California 94720*

Received October 15, 1990

Since its first demonstration (1), dynamic-angle spinning (DAS) has been successful in removing broadening in NMR spectra of solids due to first- and second-order anisotropic interactions such as chemical shielding and nuclear quadrupole coupling. In DAS, the angle of inclination of a spinning sample with respect to an external magnetic field is made time dependent, such that the evolution of anisotropic frequency components over the angles is averaged away (2, 3). Resonances from quadrupolar species such as  $^{23}\text{Na}$  and  $^{17}\text{O}$  are narrowed by an order of magnitude from those observed using conventional magic-angle spinning (MAS) techniques, and resolved isotropic peaks from crystallographically distinct nuclear sites can be observed (4, 5).

The overall shift of a resonance line observed in a DAS spectrum is the sum of two contributions, the chemical shift and the isotropic second-order quadrupolar shift, the latter depending on the strength and asymmetry of the local electric field gradients at the nucleus. The shielding and quadrupolar parameters correlate well with bond order and other structural properties, so that the narrowing of broad and often overlapping lines is useful for assigning resonances and extracting quantitative structural information. Furthermore, the inverse dependence of the second-order quadrupolar shift on the strength of the external magnetic field may be exploited to separate the shielding and quadrupolar contributions using DAS spectra obtained at different field strengths.

In a conventional DAS experiment the RF irradiation and rotor axis orientation schemes of Fig. 1 are used. For each  $t_1$  increment, two experiments, labeled a and b, are summed in order to reconstruct a "second-order echo." In a second time domain ( $t_2$ ), a free induction decay containing information about the anisotropic part of the interaction may also be acquired. Two-dimensional Fourier transformation provides a correlation of anisotropic lineshapes in the  $F_2$  frequency domain with high-resolution DAS lineshapes in  $F_1$ . Our previous implementations of DAS employed phase modulation in order to obtain quadrature detection in the first time domain, necessitating the display of the two-dimensional map as a magnitude spectrum (6). Lineshapes in both dimensions are made broader by the magnitude calculation, and the inhomogeneous powder pattern lineshapes from second-order quadrupole interactions change markedly in this mode. Here we present a scheme for obtaining pure-absorption-phase lineshapes with quadrature detection in both dimensions of a DAS experiment.

A DAS experiment may be analyzed using the coherence-transfer (CT) map (7),

\* To whom correspondence should be addressed.

also shown in Fig. 1. Evolution at  $\theta_2 = 79.19^\circ$  cancels anisotropic evolution at  $\theta_1 = 37.38^\circ$ , and no additional coherence transfer occurs after echo formation at time  $t_1$ . Only one CT pathway is retained during  $t_1$ , and phase-twisted lineshapes result. In order to obtain pure two-dimensional absorption lineshapes it is necessary to keep *both* halves of the CT pathways, i.e., both  $p = 0 \rightarrow -1 \rightarrow -1$  and  $p = 0 \rightarrow +1 \rightarrow -1$  must be present, and this does not occur in conventional DAS since there is no coherence-order change  $p = +1 \rightarrow -1$ . A similar problem is of course encountered in liquid-state spin-echo-correlated spectroscopy (SECSY) (8, 9), in which there is also no transfer of coherence after formation of the spin echo. In this case, it has been shown that the use of a z filter affects the necessary change in coherence order, allowing pure-absorption-phase spectroscopy (10). One adaptation of these ideas provides a method for pure-phase DAS and also suggests some new DAS experiments.

To accomplish pure-absorption DAS, a transfer of coherence from  $p = +1$  to  $p = -1$  at point  $t_1$  is needed. The conceptually simplest way to do this is by application of another  $90^\circ$  pulse before the beginning of  $t_2$  acquisition. Figure 2 shows schematically how this can be done with proper phase cycling and continuous spin evolution after the echo with the rotor inclined at  $\theta_2 = 79.19^\circ$ . Again, two experiments, a' and b', are necessary for each  $t_1$  point. With this simple extension of the first DAS experiment, pure-phase two-dimensional correlation is now possible with any allowable DAS angle in the second dimension. These include the angles between  $0^\circ$  and  $39.2^\circ$  or between  $63.4^\circ$  and  $90^\circ$ , as explained in Ref. (4). The fraction of time  $t_1$  spent at either angle will be different from one-half when using any set of angles other than  $37.38^\circ$  and

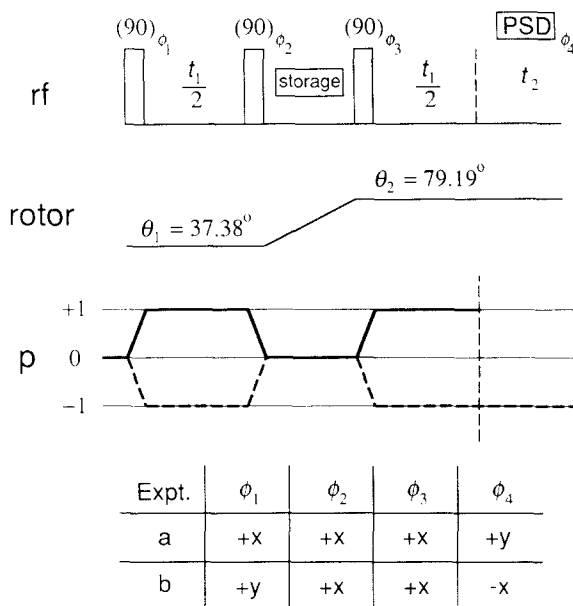


FIG. 1. RF scheme, rotor orientation, coherence order ( $p$ ), and phase cycling in a conventional DAS experiment (4). The two signals from experiments a and b are accumulated with quadrature detection according to the phase of the phase-sensitive detector (PSD) and must be summed for complete reconstruction of the second-order echo.

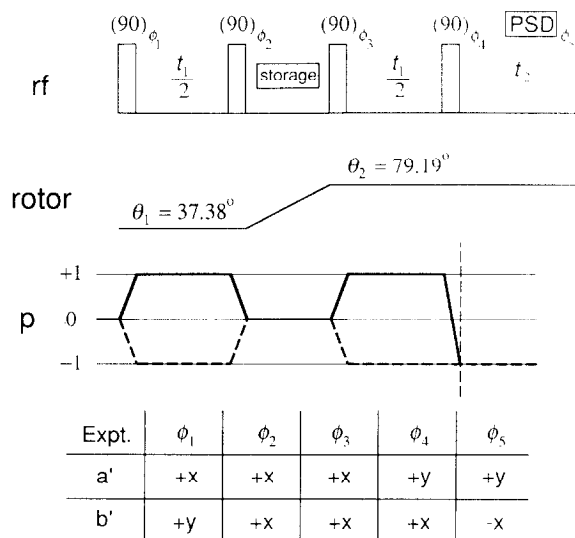


FIG. 2. New DAS experiment to accomplish pure-phase lineshapes. The fourth  $90^\circ$  pulse with phase  $\phi_4$  now transfers coherence from  $p = +1 \rightarrow -1$ , thereby retaining both coherence pathways from  $t_1$  evolution.

$79.19^\circ$ , depending on the relative magnitudes of  $P_2(\cos \theta)$  and  $P_4(\cos \theta)$  at the two angles.

At any spinning angle other than the magic angle of  $54.74^\circ$ , first-order interactions such as chemical-shift anisotropy (CSA) may be large and contribute significantly to spectral broadening in the second frequency dimension of a DAS experiment. One goal of two-dimensional DAS is to extract shielding and quadrupolar parameters associated with distinct nuclear sites by fitting simulations to single-site lineshapes extracted from slices through  $F_1$  (5). Second-order quadrupolar lineshapes may be simulated at any spinning angle  $\theta$ , neglecting CSA, and compared to experimental lineshapes in order to determine the quadrupolar coupling strength ( $e^2qQ/h$ ) and asymmetry parameter ( $\eta$ ). However, the addition of three more parameters associated with the principal values of the CSA tensor, as well as the angles describing the relative orientations of the principal-axis systems of the quadrupolar and shielding tensors, complicates analysis of the lineshapes. Hence, for optimal determination of the quadrupolar parameters and the isotropic chemical shift, especially in the presence of other anisotropic interactions, detection at the magic angle (or possibly other angles) in  $t_2$  is desirable. Because  $54.74^\circ$  is not a DAS angle, an alternative scheme using a  $z$  filter must be employed.

A  $z$  filter basically allows a single transverse magnetization component along either the  $x$  or the  $y$  axis to be retained, while eliminating the other transverse component. Effectively, it produces an overall transfer of coherence from  $p = +1 \rightarrow -1$ , not by throwing one component away along the  $z$  axis (as with a  $90^\circ$  pulse), but by storing and then reinitiating evolution of the chosen component by using two  $90^\circ$  pulses separated by a time delay  $\tau$ . One advantage of a  $z$  filter is that it should not be as sensitive to pulse imperfections as a single  $90^\circ$  pulse, since any magnetization remaining in the transverse plane after the first pulse should decay before the second pulse restores

the evolution. In addition, and most importantly, we are able to flip the rotor axis to another orientation during the delay.

Using the scheme of Fig. 3, the axis of the rotor may be reoriented, allowing detection to occur at *any* angle  $\theta_3$  with respect to the external field. Figure 3 also details the necessary phase cycling and rotor positioning. As in the previous DAS experiments only two accumulations, a" and b", are necessary to reconstruct an echo even though more pulses are required to retain the coherence order properly during  $t_1$ . The final angle  $\theta_3$  is then free for the experimenter to choose. As mentioned before,  $\theta_3 = 54.74^\circ$  will produce lineshapes in  $F_2$  that are independent of CSA, which has a larger effect at higher magnetic field strengths, and so may be the angle of choice when using DAS at higher fields. Other choices of  $\theta_3$  may include  $\theta_3 = 0^\circ$ , thereby correlating the high-resolution spectrum in the first frequency domain with static lineshapes for each distinct site, the static lineshapes being equivalent to lineshapes obtained while spinning along the  $z$  axis (11). This final angle may also be chosen with the  $90^\circ$  pulse version of the pure-phase experiment (Fig. 2) because  $\theta_2 = 0^\circ$  is complementary to  $\theta_1 = 63.44^\circ$  with an evolution period five times longer at  $\theta_2$ . The choice  $\theta_3 = 43.5^\circ$  is also useful since it has been realized that at this angle the total second-order quadrupolar linewidth is independent of the asymmetry parameter of the electric field gradient (11), so that the width is determined by the quadrupolar coupling strength, while only the shape of the line is determined by  $\eta$ .

The probe used for the DAS experiments was fabricated in the machine shop at Berkeley and is described in Ref. (12). The rotor containing the sample is held in a cylindrical stator body perpendicular to the rotor axis, and this body is flipped from

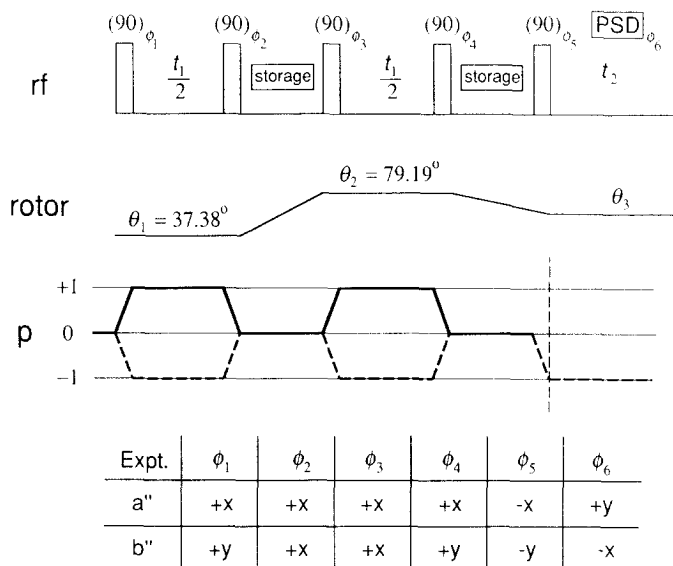


FIG. 3. A more versatile pure-phase DAS experiment, allowing axis flip to any final angle  $\theta_3$  during a  $z$  filter. The  $z$  filter mixes the two coherence orders during the flip. The time  $\tau$  for the  $z$  filter is set equal to the storage time needed for the axis flip (approximately 30 ms).

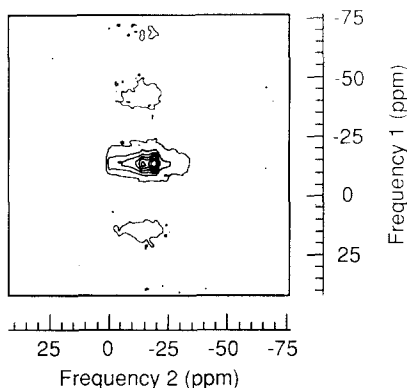


FIG. 4. Two-dimensional DAS spectrum of  $^{23}\text{Na}$  in  $\text{Na}_2\text{C}_2\text{O}_4$  using the experiment outlined in Fig. 3 for pure-phase lineshapes correlated with  $\theta_3 = 54.74^\circ$ . The  $90^\circ$  pulse times were  $8.0 \mu\text{s}$  and  $512 \times 512$  points were acquired using the method of States *et al.* (13). Two-dimensional hypercomplex Fourier transformation was performed with 30 Hz of Lorentzian line broadening in  $F_1$  and 50 Hz in  $F_2$ . A relaxation delay of 1.0 s was used, and signal averaging of 32 transients per  $t_1$  point resulted in a total experiment time of 9.3 h.

one orientation to another by a pulley coupled to a stepping motor ( $0.1125^\circ/\text{step}$  resolution) at the base of the magnet. Nominal flip times of 30 ms for a  $45^\circ$  flip are routinely accomplished. The experiments were performed in a magnetic field of 9.4 T, corresponding to a resonance frequency of 105.84 MHz for  $^{23}\text{Na}$  ( $I = \frac{3}{2}$ ). Phase-sensitive experiments can be approached with two different data accumulation and processing methods: that of States *et al.* (13), where two separate data collections for each  $t_1$  increment are performed followed by hypercomplex Fourier transformation, or by time proportional phase incrementation (TPPI) (14, 15), where only one data set is used but the phases of the first pulses in both experiments a'' and b'' are incremented by  $90^\circ$  with each  $t_1$ . In either case at least two  $t_2$  accumulations for each  $t_1$  point must always be summed to give the reconstructed second-order echo. In the former method this number is therefore doubled, as both collections for a distinct  $t_1$  must also be run with a  $90^\circ$  phase shift of the first pulses to acquire the second of the two hypercomplex data sets. To achieve the same resolution and signal-to-noise by TPPI, twice as many  $t_1$  increments must be used, thereby making equivalent the time and computer memory required for the two methods. We have tested both methods and find comparable results.

We illustrate these new ideas with the use of a z-filtered pure-phase experiment with an axis flip to  $\theta_3 = 54.74^\circ$ , corresponding to a second dimension of magic-angle spinning correlated with high-resolution DAS. The sample is sodium oxalate ( $\text{Na}_2\text{C}_2\text{O}_4$ ) and the nucleus studied is  $^{23}\text{Na}$ . Figure 4 shows a plot of the two-dimensional DAS spectrum of this compound. One-dimensional projections of this spectrum appear in Fig. 5, along with the one-dimensional MAS spectrum of the same sample for comparison. The high-resolution DAS lineshape has a width of 600 Hz, compared to an approximate MAS spectral spread of 3 kHz. Simulations with the parameters  $e^2qQ/h = 2.5$  MHz and  $\eta = 0.7$  closely match both MAS spectra. The DAS spectrum shows one isotropic peak at  $-15.0$  ppm with respect to  $^{23}\text{Na}$  in aqueous NaCl, and

thus the chemical shift may be calculated as 1.2 ppm or 127 Hz at 9.4 T. Figure 6 allows comparison of the new DAS results with projections from a magnitude calculation of phase-modulated data acquired under the same experimental conditions (number of  $t_1$ 's, scans per  $t_1$ , and spinning frequency). The pure-phase results clearly show a narrower isotropic resonance and sharper spectral features in the second frequency domain.

We note that the narrower pure-phase projection in the first frequency domain may also be recovered from the phase-modulated data set by extracting the first  $t_2$  data point ( $t_2 = 0$ ) from the anisotropic free induction decay for each  $t_1$  point. Fourier transformation of this one-dimensional decay is equivalent to the projection from the two-dimensional pure-phase experiment (compare Fig. 5c with Fig. 6c). In this case, however, there is no immediate correlation of the high-resolution line with the anisotropic lineshape, and this is especially troublesome if two lines are very near to each other in the high-resolution dimension.

In summary, we have introduced some new dynamic-angle spinning NMR experiments and have shown that pure-absorption-phase lineshapes may be obtained from consideration of the coherence-transfer pathways during an experiment. Experimental results confirm that narrower resonance lines are obtained using pure-phase mea-

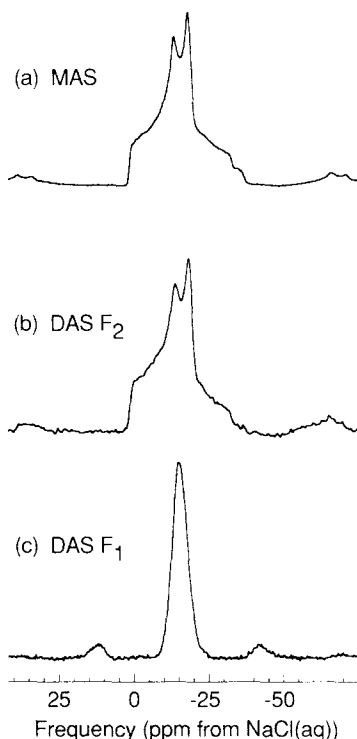


FIG. 5. (a) Magic-angle spinning (MAS) spectrum of  $^{23}\text{Na}$  in  $\text{Na}_2\text{C}_2\text{O}_4$ , showing a characteristic lineshape for  $e^2qQ/h = 2.5$  MHz and  $\eta = 0.7$  (128 transients, recycle delay = 5.0 s, pulse width ( $90^\circ$ ) = 5  $\mu\text{s}$ ). (b)  $F_2$  projection of the two-dimensional DAS spectrum of Fig. 4. (c) Projection of the high-resolution (isotropic) DAS spectrum from Fig. 4.

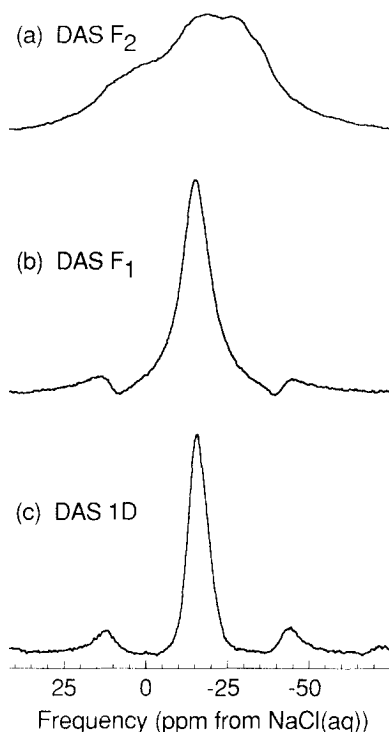


FIG. 6. (a) Magnitude-mode  $F_2$  projection from a conventional (phase-modulated) DAS experiment for  $^{23}\text{Na}$  in  $\text{Na}_2\text{C}_2\text{O}_4$ , showing a broad spectrum at a spinning angle of  $79.19^\circ$ . (b) High-resolution DAS projection from the magnitude-mode spectrum, broader than the pure-phase DAS high-resolution spectrum of Fig. 5c. (c) One-dimensional spectrum obtained from the first ( $t_2 = 0$ ) points of the phase-modulated data set. The linewidth is 600 Hz, comparable to that of the projection from the pure-phase data (Fig. 5c).

surements rather than magnitude-mode processing of data. In previous experiments, correlation of isotropic resonances in  $F_1$  has been with powder patterns obtained at the final angle  $\theta_2$ , which must lie in a specific range of DAS angles. At each possible  $\theta_2$ , line broadenings from second-order quadrupole and chemical-shift interactions are present. The particular advantage of our new experiments is that now the final angle can be selected at will, and it is possible to correlate isotropic peaks with a second frequency dimension at any angle. This makes it easier to disentangle the chemical-shift and quadrupolar contributions to the lineshape and to determine the shielding and quadrupole parameters.

#### ACKNOWLEDGMENTS

We thank G. C. Chingas for helpful discussions and J. Baltisberger for help with the simulations. K.T.M. is an N.S.F. Graduate Fellow and E.W.W. is an N.I.H. Postdoctoral Fellow. This work was supported by the Director of the Office of Energy Research, Office of Basic Energy Sciences, Materials Sciences Division of the U.S. Department of Energy, under Contract DE-AC03-76SF00098.

## REFERENCES

1. B. F. CHMELKA, K. T. MUELLER, A. PINES, J. STEBBINS, Y. WU, AND J. W. ZWANZIGER, *Nature (London)* **339**, 42 (1989).
2. A. LLOR AND J. VIRLET, *Chem. Phys. Lett.* **152**, 248 (1988).
3. A. SAMOSON, E. LIPPMAN, AND A. PINES, *Mol. Phys.* **65**, 1013 (1988).
4. K. T. MUELLER, B. Q. SUN, G. C. CHINGAS, J. W. ZWANZIGER, T. TERAQ, AND A. PINES, *J. Magn. Reson.* **86**, 470 (1990).
5. K. T. MUELLER, Y. WU, B. F. CHMELKA, J. STEBBINS, AND A. PINES, *J. Am. Chem. Soc.* **113**, 32 (1991).
6. J. KEELER AND D. NEUHAUS, *J. Magn. Reson.* **63**, 454 (1985).
7. G. BODENHAUSEN, H. KOGLER, AND R. R. ERNST, *J. Magn. Reson.* **58**, 370 (1984).
8. K. NAGAYAMA, K. WÜTHRICH, AND R. R. ERNST, *Biochem. Biophys. Res. Commun.* **90**, 305 (1979).
9. K. NAGAYAMA, A. KUMAR, K. WÜTHRICH, AND R. R. ERNST, *J. Magn. Reson.* **40**, 321 (1980).
10. O. W. SØRENSEN, M. RANCE, AND R. R. ERNST, *J. Magn. Reson.* **56**, 527 (1984).
11. F. LEFEBVRE, J.-P. AMOUREUX, C. FERNANDEZ, AND E. G. DEROUANE, *J. Chem. Phys.* **86**, 6070 (1987).
12. K. T. MUELLER, G. C. CHINGAS, AND A. PINES, *Rev. Sci. Instrum.*, submitted.
13. D. J. STATES, R. A. HABERKORN, AND D. J. RUBEN, *J. Magn. Reson.* **48**, 286 (1982).
14. G. DROBNY, A. PINES, S. SINTON, D. WEITEKAMP, AND D. WEMMER, *Symp. Faraday Soc.* **13**, 49 (1979).
15. D. MARION AND K. WÜTHRICH, *Biochem. Biophys. Res. Commun.* **113**, 967 (1983).